

Table S1.

Subject Characteristics

	Gender	Age		MELD score	
Controls n=14	F:36%(5)	46.4±3.4	F:46.8±9.4	NA	
	M:64%(9)		M:46.4±2.3		
Alcoholic cirrhosis n=28	F:21%(6)	45.7±1.4	F:44.5±2.6	<9	56.6% (15)
				10–19	35.7% (10)
	M:79%(22)		M:46±1.7	20–29	7.1% (2)
				30–39	3.6% (1)
Hepatitis B cirrhosis n=43	F:23%(10)	49.6±1.6	F:49.3±2.9	<9	67.4% (29)
				10–19	27.9% (12)
	M:77%(33)		M:49.7±1.9	20–29	4.7% (2)
				30–39	0

MELD=Model for end stage liver disease, M=male, F=female, NA=not applicable

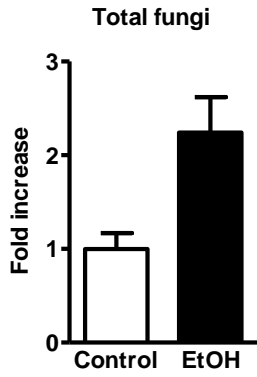
Table S2.**Subject Characteristics**

	Gender	Age		Alcoholic liver disease
Controls n=8	F:16%(2)	41.2±4.2	F:54±3	NA
	M:84%(6)		M:37±4.3	
Non-progressive alcoholic liver disease n=10	F:20%(2)	50.9±3.2	F:55±2	No liver disease (2) Mild liver disease (8)
	M:80%(8)		M:49.9±4	
Alcoholic hepatitis n=6	F:50%(3)	52.7±3.5	F:53±6.8	MELD 22±1.6
	M:50%(3)		M:52.3±4.3	
Alcoholic cirrhosis n=4	F:33%(1)	47.5±6.8	F:54	Child Pugh A (2) Child Pugh C (2)
	M:67%(3)		M:45±9.1	

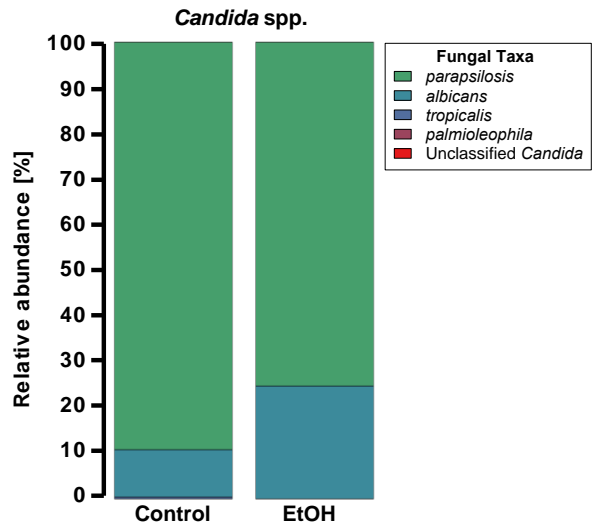
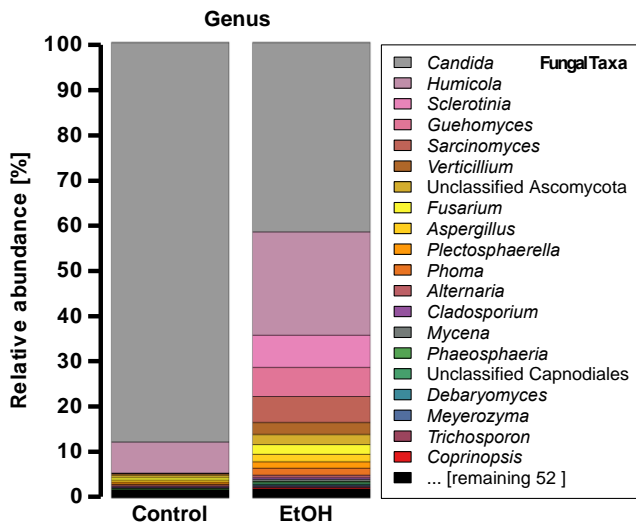
MELD=Model for end stage liver disease, M=male, F=female, NA=not applicable
Mild liver disease: AST/ALT elevation and/or hepatic steatosis on imaging

Figure S1

A



B



C

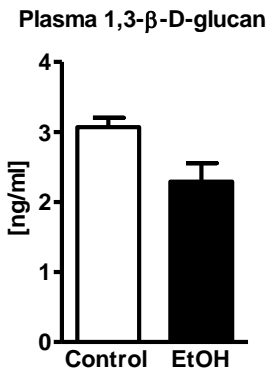


Figure S1

Figure S1. Changes in the intestinal mycobiota and translocation of fungal products following chronic alcohol feeding. (A and C) C57BL/6 mice were fed an oral control diet (n=4–5) or ethanol diet (n=4–14) for 5 weeks. Total fungi in feces were assessed by qPCR (A), and mean plasma levels of 1,3- β -D-glucan were measured by ELISA (C). (B) ITS sequencing of fecal samples from C57BL/6 mice that were fed an oral control diet (n=9) or ethanol diet (n=9) for 8 weeks. The graph demonstrates the average relative abundance of sequence reads in each fungal genus (left panel) and *Candida* species (right panel) for control and for ethanol-fed mice. Unpaired Student *t* test.

Figure S2

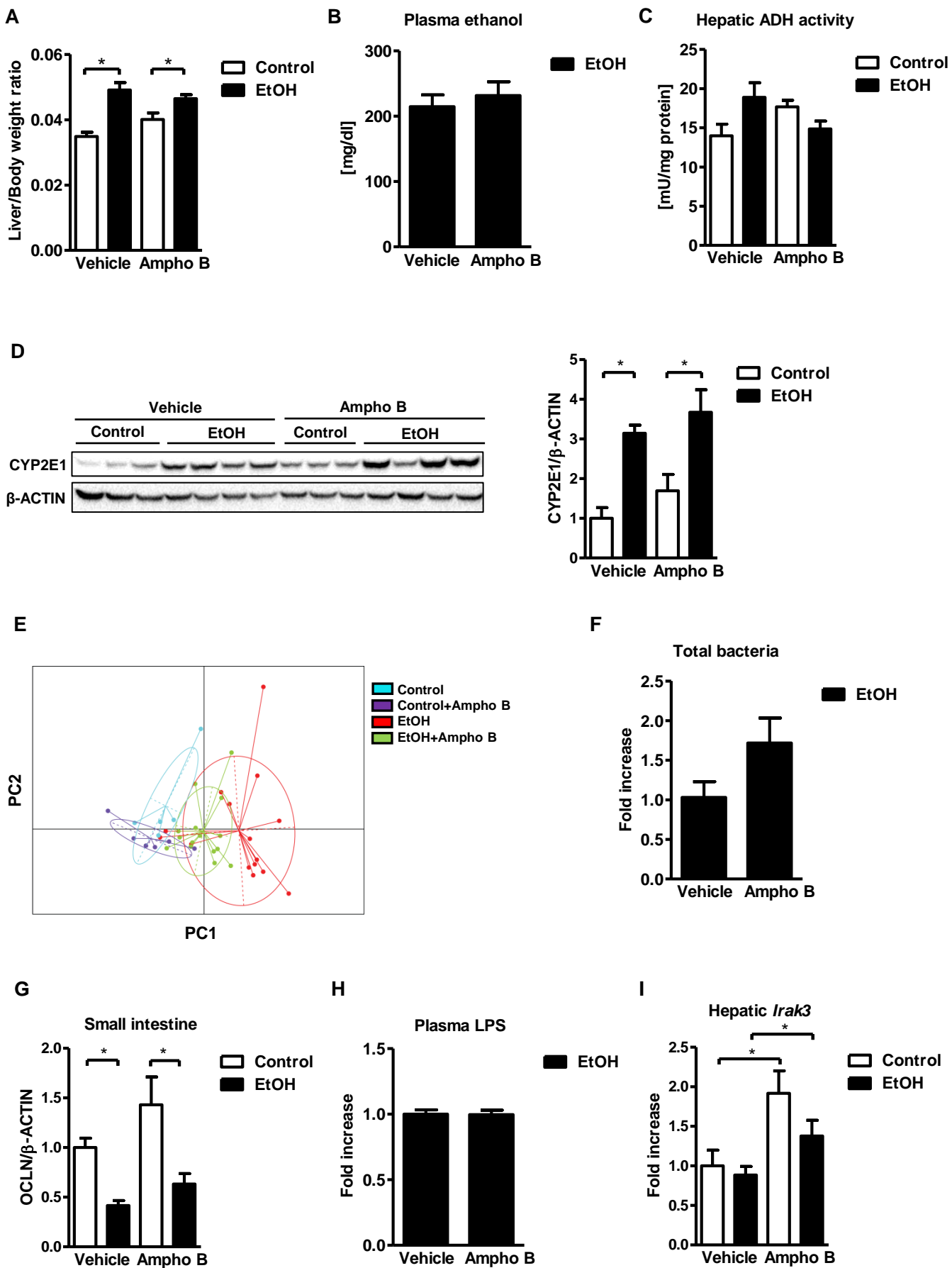
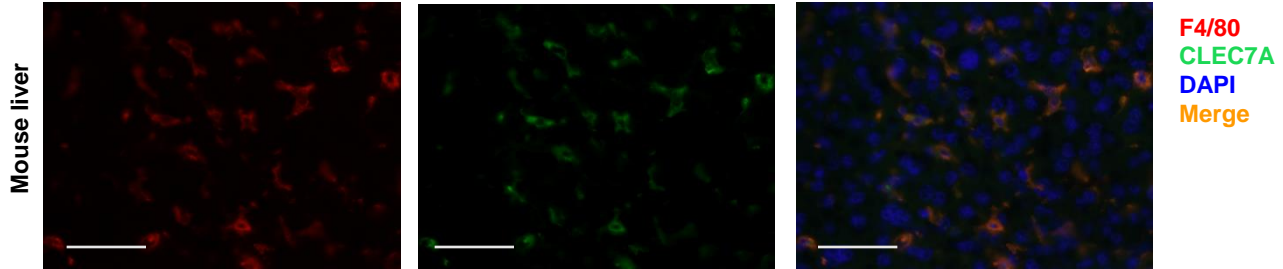


Figure S2

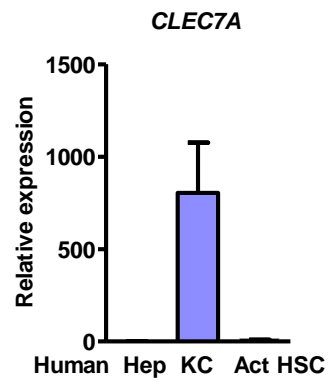
Figure S2. Absorption and hepatic metabolism of ethanol. C57BL/6 mice were fed an oral control diet (n=5–6) or ethanol diet (n=12–15), and also given vehicle or amphotericin B (Ampho B). (A) Ratio of liver to body weight. (B) Plasma level of ethanol at time of harvesting. (C) Hepatic ADH activity. (D) Immunoblot analysis of hepatic CYP2E1 (n=5 for mice fed a control diet, n=8 for mice fed an ethanol diet). (E) Principal component analysis (PCA) of bacterial microbiomes. (F) Total bacteria in feces were assessed by qPCR. (G) Immunoblot analysis of OCLN (occludin) in the small intestine (n=5 in each group). (H) Plasma LPS. (I) Hepatic expression of *Irak3* mRNA. Unpaired Student t test. * $P < .05$.

Figure S3

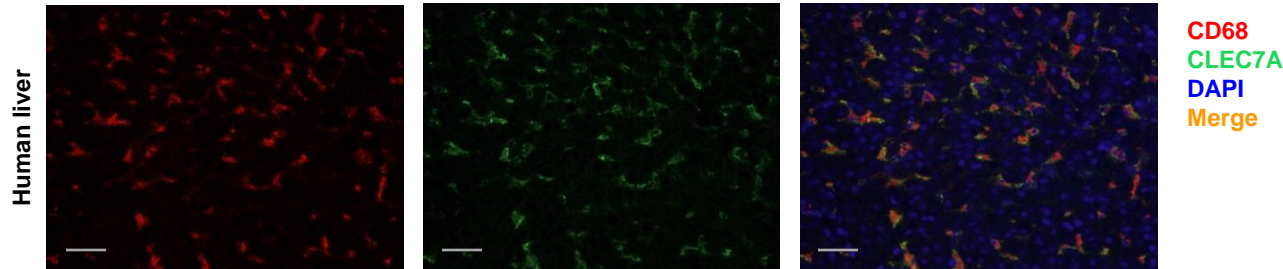
A



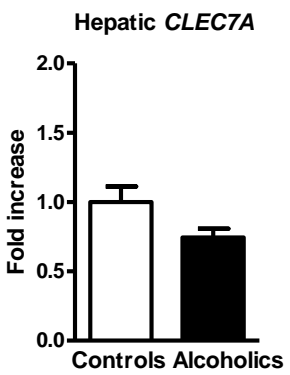
B



C



D



E

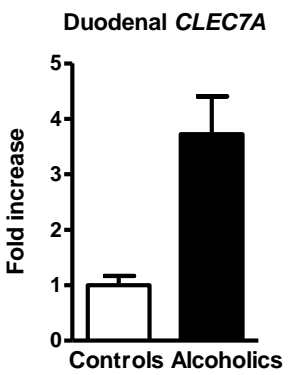


Figure S3

Figure S3. Expression of CLEC7A. (A) Immunofluorescence analysis of F4/80 (red) and CLEC7A (green) in non-diseased mouse liver (representative liver sections); nuclei are blue. (B) Expression of *Clec7a* in primary human hepatocytes (Hep), Kupffer cells (KC), and activated hepatic stellate cells (Act HSC) was measured by qPCR (n=2 independent experiments). (C) Immunofluorescence analysis of CD68 (red) and CLEC7A (green) in non-diseased human liver (representative liver sections); nuclei are blue. (D) Expression of *CLEC7A* mRNA in hepatic biopsies from controls without alcohol dependency (n=9) and alcohol-dependent patients (n=65). (E) Expression of *CLEC7A* mRNA in duodenal biopsies from controls without alcohol dependency (n=12) and alcohol-dependent patients (n=110). Scale bars, 50 μ m. Unpaired Student t test. * P <.05.

Figure S4

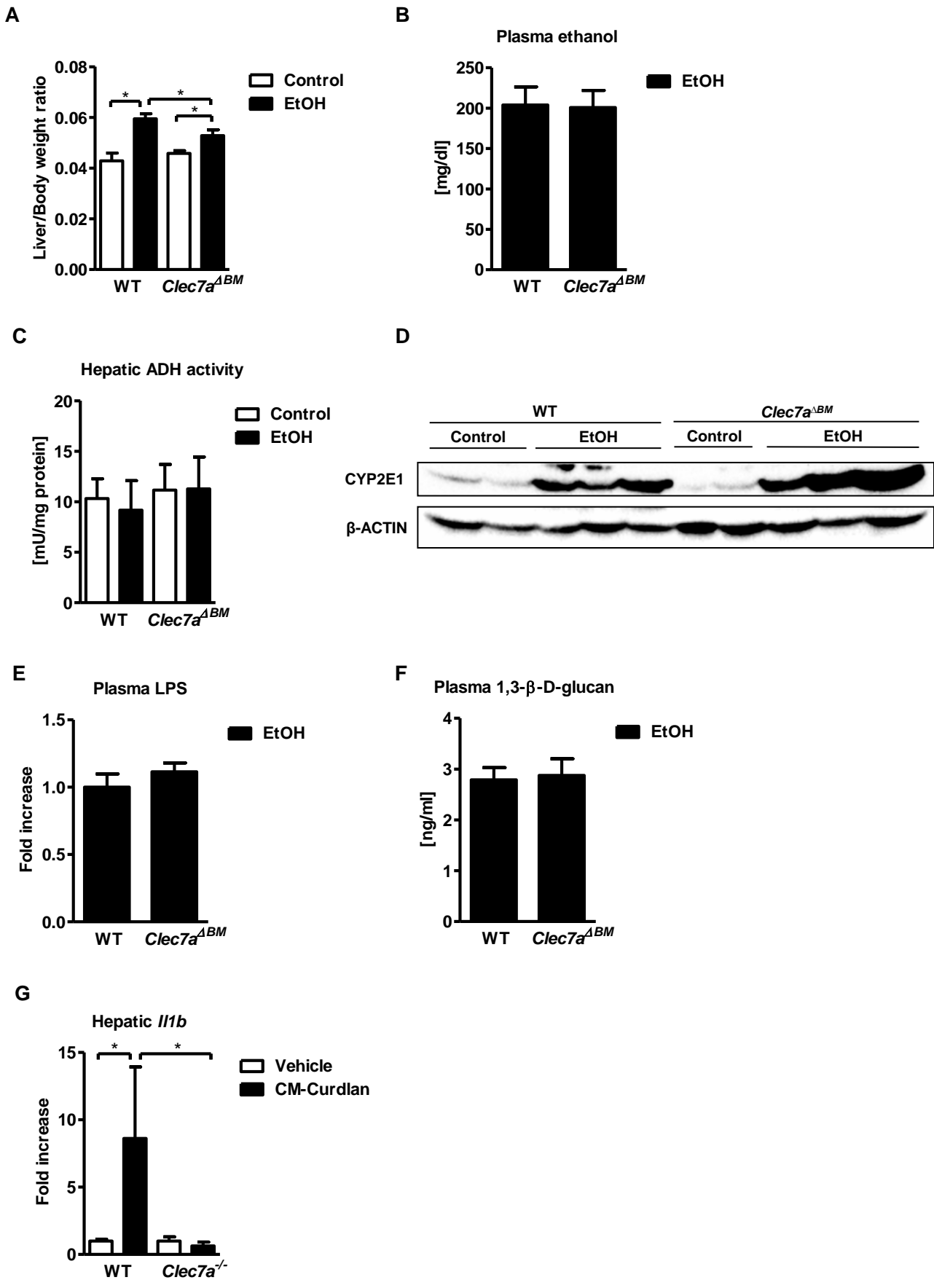


Figure S4

Figure S4. Absorption and hepatic metabolism of ethanol. C57BL/6 mice were transplanted with bone-marrow from WT (WT) or *Clec7a*^{-/-} mice (*Clec7a*^{ΔBM}) and fed an oral control diet (n=4–5) or ethanol diet (n=6–10). (A) Ratio of liver to body weight. (B) Plasma level of ethanol at time of harvesting. (C) Hepatic ADH activity. (D) Immunoblot analysis of hepatic CYP2E1. (E) Plasma LPS. (F) Plasma 1,3-β-D-glucan. (G) Hepatic expression of *Ii1b* mRNA in WT (n=6) and *Clec7a*^{-/-} mice (n=3) 2hrs after intraperitoneal injections with carboxymethyl-β-1,3-D-glucan (2mg/mouse). Unpaired Student *t* test (A–C, E–G). Mann-Whitney U-statistic test (H). **P*<.05.

Figure S5

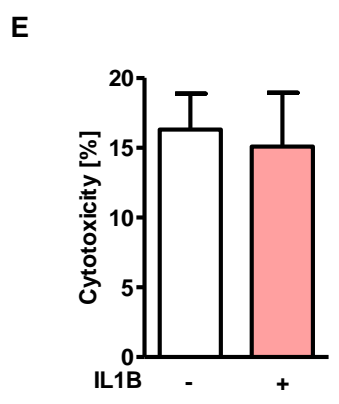
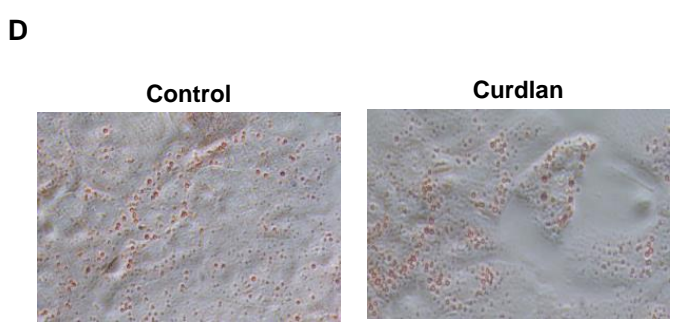
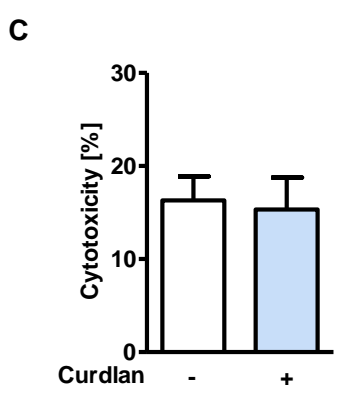
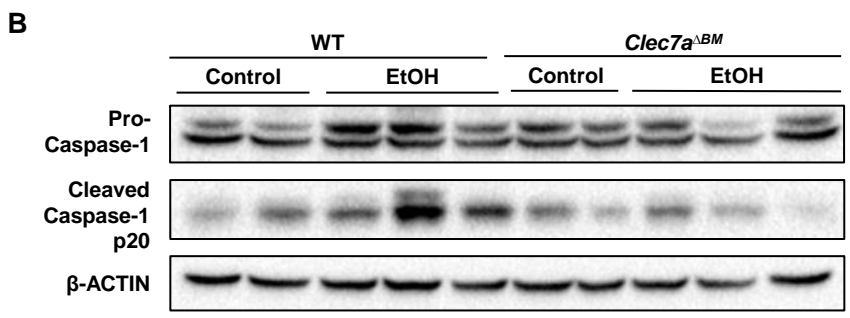
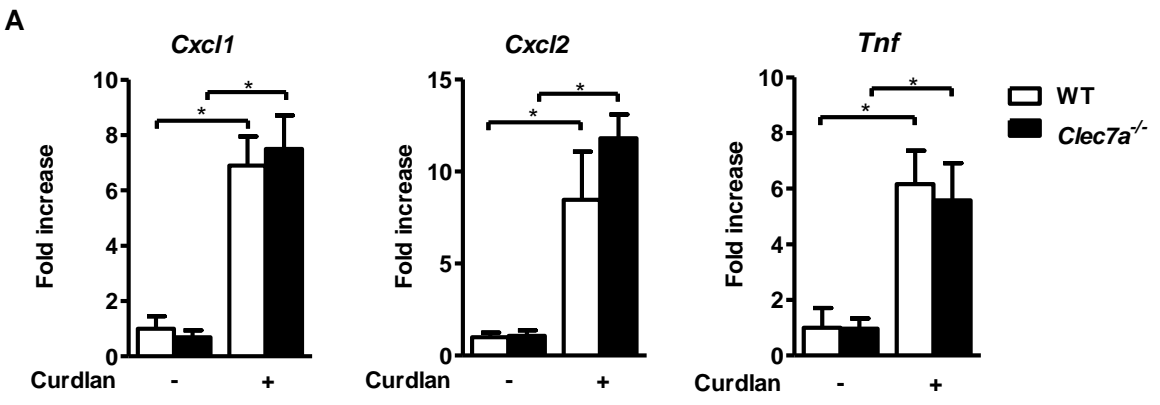


Figure S5

Figure S5. Curdlan does not induce hepatocyte death or steatosis. (A) Primary mouse WT and *Clec7a*^{-/-} Kupffer cells were stimulated with curdlan; graphs show expression of *Cxcl1*, *Cxcl2* and *Tnf* mRNA (n=4–6 independent experiments). (B) C57BL/6 mice were transplanted with WT (WT) or *Clec7a*^{-/-} bone-marrow (*Clec7a*^{ΔBM}) and fed an oral control diet or ethanol diet. Hepatic caspase-1, cleaved caspase-1 and β-actin protein. (C–D) Hepatocytes were stimulated with curdlan. Hepatocyte cytotoxicity (C) and lipid accumulation as determined by Oil Red O-staining (D); n=3 independent experiments. (E) Hepatocytes were stimulated with IL1B and hepatocyte cytotoxicity measured; n=3 independent experiments. Unpaired Student t test. **P*<.05.

Figure S6

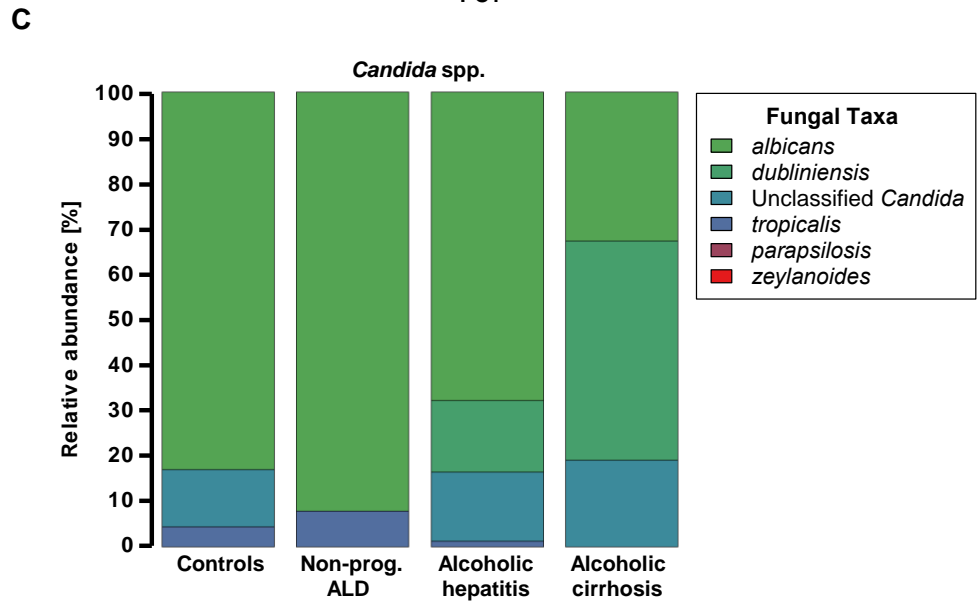
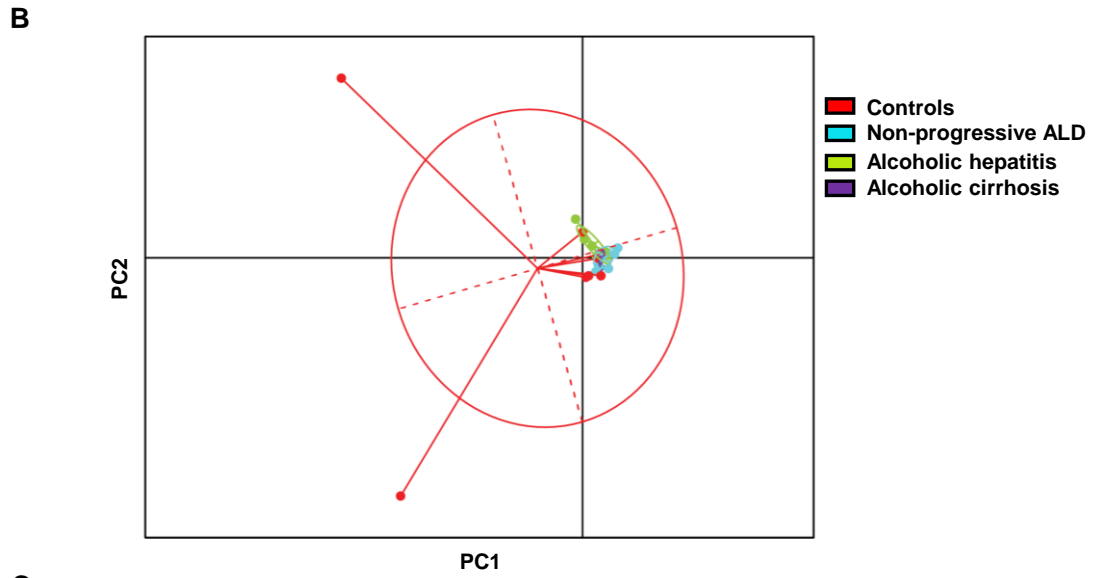
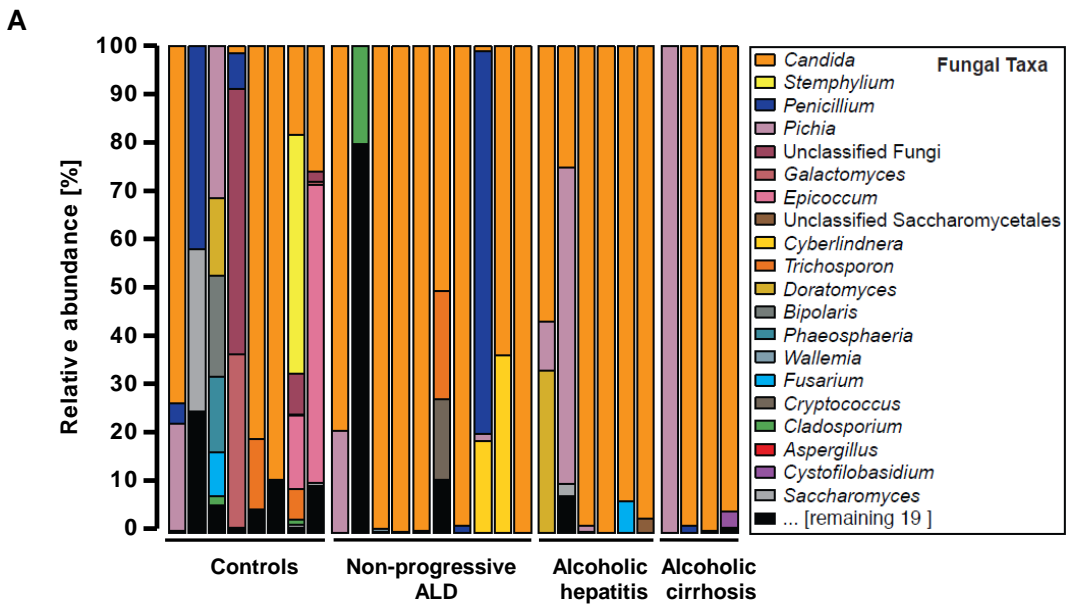


Figure S6

Figure S6. Intestinal fungal dysbiosis in patients with alcohol abuse. ITS sequencing of fecal samples from controls (controls, n=8) or alcohol-dependent patients with non-progressive alcoholic liver disease (non-progressive ALD, n=10), alcoholic hepatitis (alcoholic hepatitis, n=6), or alcoholic cirrhosis (alcoholic cirrhosis, n=4). (A) The graph demonstrates the relative abundance of sequence reads in each genus for each individual person. (B) PCA of mycobiomes. (C) *Candida* species composition of human fungal ITS sequences from Fig. 6A divided into four groups: (controls; n=8), alcohol-dependent patients with non-progressive alcoholic liver disease (non-prog. ALD; n=10), alcoholic hepatitis (alcoholic hepatitis; n=6), or alcoholic cirrhosis (alcoholic cirrhosis; n=4).